Published in final edited form as:
Laryngoscope. 2010 October ; 120(10): 2047–2053. doi:10.1002/lary.21106.

Hearing Loss Alters Quantal Release at Cochlear Nucleus Stellate Cells

Alexander W. Rich, M.D.[1], **Ruili Xie, Ph.D.**[1], and **Paul B. Manis, Ph.D.**[1,2]

[1] Department of Otolaryngology/Head & Neck Surgery, University of North Carolina, Chapel Hill, North Carolina, U.S.A

[2] Department of Cell and Molecular Physiology, University of North Carolina, Chapel Hill, North Carolina, U.S.A

Abstract

Hypothesis—Auditory nerve synapses in ventral cochlear nucleus end on two principal cell types, bushy and stellate cells. While the effects of hearing loss on bushy cells has been well studied, little is known about the effects of hearing loss on synaptic input to the stellate cells. Based on prior observations in bushy cells, we hypothesized that noise-induced hearing loss (NIHL) would decrease quantal release onto stellate cells.

Study Design—Prospective, randomized animal study.

Methods—CBA/CaJ mice were exposed for 2 hours to 98dBSPL 8–16kHz noise to produce a temporary threshold shift (TTS), or 114dBSPL to produce a permanent threshold shift (PTS). Spontaneous miniature excitatory postsynaptic currents (mEPSCs) were then measured in stellate cells in brain slices of the cochlear nucleus.

Results—Click-evoked auditory brainstem evoked response thresholds were elevated by 35dB in both TTS and PTS mice. Spontaneous mEPSC frequency was found to be five-fold higher than normal in stellate cells of TTS mice and 3-fold higher in PTS mice. mEPSC amplitude was also larger in PTS mice. The mEPSC time course was not different between experimental and control groups.

Conclusions—The dramatic increase in mEPSC frequency after NIHL was not expected. The increase in mEPSC amplitude in PTS mice suggests a post-synaptic remodeling process. Both of these effects could contribute to increased spontaneous firing in the cochlear nucleus in the absence of sound. Our results also suggest that hearing loss may have different effects at auditory nerve synapses on bushy and stellate cells in the VCN.

Level of Evidence—Not applicable.

Introduction

Hearing loss affects over 28 million people in the United States, with approximately 10 million of those having noise-induced hearing loss (NIHL)1. NIHL is rapidly becoming a greater concern as more people live in urban, acoustically-enriched environments for extended periods2. Additionally, the increase in NIHL correlates with an increasing prevalence of tinnitus. NIHL is primarily, though not exclusively, caused by damage to or

Address for Correspondence: Dr. Paul B. Manis, Dept. of Otolaryngology/Head and Neck Surgery, G127 POB, CB#7070, 170 Manning Drive, University of North Carolina at Chapel Hill, Chapel Hill, NC 27599-7070, pmanis@med.unc.edu, Tel: (919) 966-8926, Fax: (919) 966-7941.

Conflict of Interest: The authors have no conflict of interest to disclose or declare with regards to this work.

loss of hair cells within the cochlea3, 4. In response to the decreased sensory input, the central nervous system undergoes both degenerative and homeostatic compensatory changes that alter sensory function. After transduction of sound into neural impulses in the cochlea, the information carried in the auditory nerve (AN) is transformed by synapses onto the different cell types in the cochlear nucleus. In the ventral cochlear nucleus (VCN), there are two principal cell types, called bushy and stellate cells, respectively5. These cells are innervated by the AN in different ways, have different expression of ion channels and intrinsic electrical activity6, 7, and their responses to sound convey different information8. The anatomic structure of these cells and pathways is conserved in mammals 5, including humans 9, 10, and the physiological responses of the cells to sound is similar in mice, guinea pigs, cats 11–13 and primates (both old and new world monkeys) 14. Thus lower mammals, including mice, are excellent models for understanding central responses to hearing loss.

While the bushy cells convey fine temporal information, the stellate cells convey information about stimulus intensity and stimulus envelope (amplitude modulation) 11, 15, 16. Stellate cells play an important role in auditory perception, since speech recognition can take place in the absence of fine temporal or spectral information by using slower amplitude modulation, or envelope, cues 17, and thus does not require the specializations present in the bushy cell pathways (although bushy cells can also encode those cues). Many studies have examined the consequences of hearing loss by cochlear ablation or genetics on transmission at the end bulb of Held synapses on bushy cells, but fewer have examined the effects on stellate cells.

Miniature EPSCs (mEPSCs) are thought to represent the release of a single vesicle from a presynaptic terminal, and represent the fundamental unit (quanta) of synaptic transmission. mEPSCs occur spontaneously (sEPSCs) at synapses in the absence of presynaptic action potentials. Changes in sEPSC frequency and amplitude have been described in the VCN in response to changes in auditory input. In bushy cells from the high-frequency region of the VCN, animals with an age-related, high frequency hearing loss show a decreased sEPSC frequency, and the events become slower and smaller18. In contrast, the frequency of sEPSCs in VCN stellate cells does not increase during development, nor is it affected by cochlear ablation during the critical period of hearing onset 19 (following cochlear ablation, the synaptic inputs driving these sEPSCs must come from a source other than the AN). The intrinsic physiology (input resistance, spike shape) of rat stellate cells is also little affected by cochlear ablation 20. In deaf jerker mice, which never develop normal hearing, the frequency of sEPSCs in stellate cells is higher than in wild-type 21. NIHL may involve or engage different mechanisms than genetic or developmentally related, or cochlear ablation induced hearing loss, even though from the standpoint of the central auditory system sound-evoked activity is ultimately reduced. We therefore tested the hypothesis that NIHL, by decreasing auditory nerve activity, would result in decreases in transmission in VCN stellate cells similar to those seen in age-related high frequency hearing loss in bushy cells. To test this idea, we characterized mEPSCs in mouse VCN stellate cells in two NIHL models.

Methods

Experimental Animals

CBA/Caj mice between 25 and 40 days old were used in this study. All animal protocols were approved by the Institutional Animal Care and Use Committee at the University of North Carolina at Chapel Hill (protocol numbers 06–227 and 09–223). Care was taken to minimize the number of animals needed for experimentation. For auditory brainstem evoked response (ABR) testing and brain slice preparation, all animals were anesthetized with 100mg/kg ketamine and 10mg/kg xylazine until are flexic to deep paw pinches.

Noise Exposure

Mice, aged postnatal days (P) 25–P30, were divided into three groups. Control mice received no noise exposure. A second group of mice was exposed to digitally generated octave band noise from 8–16 kHz, filtered with 8-pole elliptical filters, over a period of 120 minutes, at 98 dB SPL. This exposure protocol was used to generate a temporary threshold shift (TTS) that recovered to within 5 dB of pre-exposure threshold levels after 2 weeks. The third group of mice received the same noise exposure, except that the stimulus level was increased to 114 dB SPL to induce a permanent threshold shift (PTS). Mice were exposed in a reverberant sound box where they were free to move during the noise exposure, but were restricted to a small area within a mesh cage suspended in the center of the box. Following the noise exposure, the mice were returned to the animal housing facility until they underwent terminal experiments (24 hr for TTS mice and 2 weeks for PTS mice). The noise stimulus was generated in MATLAB (V7.6, The Mathworks, Natick, MA), delivered through a 16-bit D/A (National Instruments, Arlington, TX, NI 6731) card at 500 kHz through a Crown D75-A amplifier and a Selenium (Nova Santa Rita, Brazil) D-3300 Ti speaker. The sound level in the reverberant box was measured with an ACO-Pacific (Belmont, CA) 0.5-inch microphone, and referenced to an ACO-Pacific 521 sound level calibrator.

ABR testing

The hearing status of each animal was determined prior to brain slice preparation. Each mouse was anesthetized as described above and a 1 mm incision made in the lateral aspect of the tragus to allow for better access of the external auditory canal. The mouse was then placed in an acoustically isolated chamber on a heating pad and maintained at 37°C via a thermostatically controlled feedback system (Harvard Apparatus, Holliston, Massachusetts). An ES-1 electrostatic speaker (Tucker-Davis, Gainesville, FL) with a1.5 cm polyethylene tube was inserted into the external auditory canal to create a closed acoustic system. Recording electrodes were placed at the vertex and the mastoid, while the reference electrode was placed in the rump area. Signals were amplified 10,000x and bandpass filtered from 300–3000 Hz. ABR responses were averaged with a Tucker-Davis (Gainesville, FL) System-3 RP2.1 processor controlled by a MATLAB program. Stimuli were generated by an NI6731 D/A card at 500 kHz, and passed through a PA5 attenuator prior to delivery to the electrostatic speaker amplifier. A series of responses to clicks (monophasic, 100 μsec duration) were collected at 5 dB intensity increments with a maximum intensity of 80 dB SPL. The click polarity (rarefaction or condensation) alternated on sequential trials to cancel the cochlear microphonic. Responses to 500 stimuli were averaged, ABRs were analyzed by plotting the amplitude of each peak against stimulus intensity. Thresholds were determined either by visual inspection orusing an automated algorithm. The automated algorithm measured the ABR signal energy in an 800–1200 Hz spectral window, and threshold was set as the stimulus level at which the energy in this window exceeded 2 standard deviations of the energy in the recording noise floor. Threshold determined in this way were consistent with those from visual inspection.

Slice preparation

Following the ABR, supplemental anesthesia was given if needed, the mouse was decapitated, and the brainstem (including the cochlear nucleus) was harvested. The tissue was then immersed in pre-warmed (34°C) artificial cerebrospinal fluid (ACSF), which contained (in mM): 122 NaCl, 3 KCl, 1.25 $KH2PO_4$, 20 glucose, 25 $NaHCO_3$, 2 Na-pyruvate, 3 myo-inositol, 0.4 ascorbic acid, 2 $CaCl_2$, 2 $MgSO_4$, and was bubbled with 95% O_2 and 5% CO_2 to a pH of 7.4. Tissue blocks containing the cochlear nucleus were then trimmed and mounted on a Leica VT1000S vibratome (Banockburn, IL). A 300μm parasagittal slice containing the cochlear nucleus was then cut and incubated for at least 30

minutes at 34°C prior to beginning recordings. Since the cochlear nucleus protrudes from the lateral aspect of the brainstem, the slices contained principally the cochlear nucleus 18, 22, and small adjacent areas of the brainstem and cerebellum. The cochlear nucleus was readily identifiable in these parasagitttal slices by the entry point of the auditory nerve, the pattern of myelin fasciculation in the anterior portion of the nucleus, and the characteristic lamination of the dorsal cochlear nucleus. The slices were secured in the recording chamber with a nylon net, with continuously flowing ACSF at 5 mL/min. In order to block inhibitory post-synaptic currents, 2μM strychnine was added during all recordings.

Recording

Whole-cell patch electrode pipettes (3–8 MΩ) were pulled from 1.5mm borosilicate KG-33 glass (Garner, Claremont, CA) with a Sutter P2000 puller (San Francisco, CA) and were then coated with Sylgard184 (Dow Corning, Midland, MI) before use. Pipettes were filled with (in mM) 125 $CsMeSO_3$, 15 CsCl, 5 ethyleneglycol-bis-(aminoethyl ether)-N,N,N′,N′-tetra-acetic acid (EGTA), 10 N-2-hydroxyethyl-piperazine-N--2-ethane-sulphonate(HEPES), 4 Mg adenosine triphosphate, 10 creatinine phosphate, 0.3 guanosine triphosphate, and 3 QX314. Cesium and QX314 were used to block K^+ and Na^+ conductances, respectively. The pH was adjusted to 7.2 with CsOH and the osmolarity was set to 290 mOsm. AlexaFluor 488 (In Vitrogen, Carlsbad, CA) was added to the pipette to visualize cellular morphology. Under fluorescence, stellate cells were identified by their long and smooth dendrites while bushy cells showed short and heavily-branched dendrites 23. Whole-cell recordings and were made using a Multiclamp 700B amplifier (MDS Analytical Technologies, Toronto, Ontario, Canada). Data were collected using an in-house program written in MATLAB.

Data Analysis

mEPSCs were detected with a template-matching algorithm implemented in MATLAB24,18. mEPSCs frequency, amplitude, 10–90% rise time, and decay time constant were measured from the averaged events in each cell. Statistical significance ($p<0.05$) was determined using unpaired Student's t-test, or with a 1-way ANOVA followed by a Bonferroni post-test to correct for multiple comparisons. All statistical analyses were performed using Prism 5.0 (GraphPad, La Jolla, CA). Data are shown as means ± SEM.

Results

Noise-induced hearing loss

Acceptable recordings of sufficient duration for data analysis were obtained from 32 cells in 32 animals (11 control cells, 11 cells in TTS mice, and 10 cells in PTS mice). To confirm that our control mice had normal hearing, the ABRs of non-noise exposed CBA/CaJ mice between the ages of 26–40 days were measured. The mean threshold (in dB SPL) in response to click stimuli was 43.1±1.1 (n=11), which was not greatly different from 37±3 dB SPL, as reported previously25. This mean threshold was compared to the thresholds of TTS mice 1 day after noise exposure, TTS mice 10–14 days after noise exposure, when the threshold shifts should have recovered, and PTS mice 10–14 days post-noise exposure (Fig. 1).

One day post-exposure, mice in the TTS group had a mean click threshold of 75.3±2.2 dB SPL (n=11), which was significantly higher than that of the control group ($p <0.0001$). Mice in the PTS group had a mean click threshold of 74.6±1.2 dB SPL (n=10), which was also significantly higher than the control group ($p <0.0001$), but was not significantly different from the TTS group one day after exposure ($p=0.14$). A separate subgroup of TTS mice tested at 10–14 days post-exposure had a mean threshold of 46.8±2.7dB SPL (n=5), which

was not significantly different from the control group (p=0.10), demonstrating that the lower level of noise exposure produced a temporary threshold shift that recovered, as intended.

sEPSC frequency is increased in TTS and PTS CBA/CaJ mice

sEPSCs were recorded for 50s in blocks for each stellate cell while the cell membrane was held at −70 mV. Representative traces are shown for the control mice, TTS mice, and PTS mice in Figure 2A. The frequency of sEPSCs in the TTS animals was on average 5.7 times larger than in the control group (Control: 1.8±0.3 Hz, n=11; TTS: 10.1±2.8 Hz, n=11; p=0.0055) (Fig. 2B). In addition, the frequency of sEPSCs in the PTS animals was 3.8 times larger than in the control (PTS: 6.7±1.8Hz, n=10; p=0.0063) (Fig. 2B). The difference in frequency of events between PTS mice and TTS mice was not statistically significant (p=0.167; Fig 2B.) These results indicate that the noise exposure resulted in large increases in the rate of spontaneous release of transmitter in single-vesicle packets (quanta) from the excitatory auditory nerve terminals onto stellate cells.

sEPSC amplitude is increased in PTS mice but not in TTS mice

The amplitude of sEPSCs in PTS mice was 1.3 times larger than in control animals (Control: 55.3±5.5 pA, n=11; PTS: 71.3±6.4 pA, n=10; p=0.037) (Fig. 3). The amplitude of sEPSCs (60.9±4.8pA, n=11) in the TTS group was not significantly different from that of the control group (p=0.23), but was also not significantly different from that of the PTS group (p=0.10). These results suggest long term, post-synaptic changes in the mice with permanent threshold shifts.

sEPSC time course is not affected by NIHL

There was no difference in the 10–90% rise time between the control and the TTS mice (Control:0.11±0.01 ms, n=11; TTS: 0.10±0.01 ms, n=11; p=0.31), or the control and PTS mice(PTS: 0.12±0.015, n=10; p=0.16), or TTS vs. PTS (p=0.10) (Fig. 4A). There was also no significant difference between the falling time constant of the means EPSCs in the control and TTS groups (Control: 0.48±0.04 ms, n=11; TTS: 0.48±0.06 ms, n=11; p=0.49) (Fig. 4B). Although there was a trend towards a longer decay time constant in the PTS mice, the difference was not significant when compared to either the control group (PTS: 0.68±0.12, n=10; p=0.057vs. control) or TTS group (p=0.071vs. control). These findings suggest that the AMPA receptor subunit composition was most likely unchanged at these synapses after NIHL.

Discussion

We investigated sEPSCs in VCN stellate cells from normal mice and in mice that received noise-exposure to generate either TTS or PTS. The frequency of sEPSCs was dramatically higher in TTS and PTS mice than in control animals. Furthermore, we showed that the amplitude of these events was significantly larger in PTS mice than in unexposed mice, but not significantly higher than the TTS mice. No significant changes in sEPSC 10–90% rise time or decay time constant were noted between the three experimental groups. These results differ from previous studies on synaptic changes during early-onset hearing loss and cochlear ablation (as discussed below), which suggests that there are different mechanisms underlying sEPSC changes in stellate cells in response to noise exposure. Furthermore, our data suggest that there are different responses to hearing loss in the sEPSC shapes of VCN bushy and stellate cells.

We have called the events we measure sEPSCs because we did not block potential presynaptic action potentials. However, the sEPSCs are very likely to be composed solely of mEPSCs (e.g., spontaneous quantal release events) for two reasons. First, the auditory nerve

was cut in this preparation, and there is no evidence that the transected nerve fibers are themselves spontaneously active. If they were, we would expect to see some evoked EPSCs, which are typically more than 4 times larger than the sEPSCs we have recorded. The absence of spontaneous firing in the auditory nerve is also supported by the lack of even larger EPSCs in bushy cells under similar conditions18, and the lack of an effect of tetrodotoxin on the amplitude sEPSCs in either bushy cells or stellate cells26, 27.

The frequency and amplitude of stellate cell mEPSCs in normal mice has been described previously. Gardner et al26 recorded from T-stellate cells from inbred CBA and ICR mice (p18–p25), and observed sEPSCs with a frequency 3±2 Hz and an amplitude of 88±59 (±SD) pA (n=6). Conversely, a study using C57BL/6 mice observed sEPSCs at 1.5±2.0 (±SD) Hz and with an amplitude of 53±17 (±SD) pA at age P21 (n=9)19. These observed frequencies in both studies are similar to our control group, although the amplitude of sEPSCs in the Gardner study were somewhat higher than in our study. Differences in electrode solutions, recording temperature, and voltage-clamp compensation methods between the studies are likely to contribute to this difference.

Changes in stellate cell sEPSCs with hearing loss differs depending on the type of hearing loss. In the posterior VCN of congenitally deaf *Espn*^{je} mice21, sEPSC frequency was found to be significantly higher than wild-type mice ($p < 0.005$), although no other sEPSC attribute was affected. In contrast, cochlear ablation at P7 or P14 did not produce any significant changes in stellate cell mEPSC frequency, amplitude or time course19. However, in this situation, the mEPSCs must arise from non-auditory nerve synapses. When compared to our findings of significantly greater sEPSC frequency in TTS and PTS mice, and of greater sEPSC amplitudes in PTS mice, it would seem that there are different mechanisms underlying pre-and post-synaptic changes in response to different kinds of hearing loss in stellate cells.

NIHL induces both pre-and post-synaptic changes in AN transmission to VCN stellate cells

The dramatic increase in sEPSC frequency in VCN stellate cells following noise exposure could arise from several different mechanisms. While the exact mechanisms controlling spontaneous vesicle release are not fully understood, the increase that we observed could result from either activity-dependent or homeostatic changes that ultimately influence the spontaneous release processes. For example, both basal calcium and brain-derived neurotrophic factors have been shown to regulate spontaneous transmitter release at central synapses28, 29. An alternative possibility is rapid sprouting of auditory nerve fiber terminals in the VCN, leading to more terminals that are releasing transmitter onto a given target cell. There is emerging evidence that axonal growth plays a role in both the afferent and efferent auditory pathway in response to peripheral damage. For example, GAP-43, a protein associated with neuronal growth, is upregulated in the VCN after cochlear ablation30. On the other hand, an increase in synapse number due to sprouting seems unlikely in the time frame of our experiments, as immunostaining for synaptophysin, a protein found in presynaptic terminals, decreases for 7–14 days following acoustic trauma in the chinchilla VCN 31. This result suggests that there is a decrease, rather than an increase, in the number of terminals. At least within the 2-week time frame of the PTS in our study, this finding seems to be inconsistent with a sprouting hypothesis. Additionally, the rapid changes seen in TTS mice seem very unlikely to be driven by terminal sprouting but are more likely result from intrasynaptic mechanisms secondary to a rapid loss (after just several hours) of afferent presynaptic input from the inner hair cells of the cochlea32.

The increase in sEPSC amplitude in the PTS model is likely to reflect a change in AMPA receptors. Increases in AMPA receptor currents and changes in receptor composition with hearing loss models have been previously reported 18, 33, 34. It is interesting that this

increase is only seen in the PTS model, which may reflect a delayed post-synaptic response to the decrease in afferent input.

Classic studies suggest that hearing loss from cochlear ablation results in a loss of spontaneous activity in the auditory nerve as well as in the ventral cochlear nucleus35. However, the effects of noise induced hearing loss alone have not been carefully studied. Our results indicate that the frequency of spontaneous synaptic inputs to the VCN stellate cells is significantly increased following intense noise exposure. Stellate cells have relatively high input resistances, up to 150 MΩ7, 36, so individual sEPSCs are estimated to be 1–2 mV in amplitude. Such events occurring at a high rate with a Poisson-like event interval distribution should occasionally summate to cause spontaneous action potentials. Whether the high rate of sEPSCs alone would be sufficient to produce a percept is not clear, since the activity in individual cells would most likely not be correlated with firing in other cells. On the other hand, if some spontaneous activity remains in the innervating auditory nerve fibers after the noise exposure, the increased spontaneous mEPSCs could be additive to evoked EPSCs, including those that are sub-threshold, leading to recruitment37 and an increase in spontaneous firing rates. In the dorsal cochlear nucleus, NIHL increases spontaneous firing rates38, which in turn has been associated with the generation of tinnitus. Whether spontaneous rates increase in the VCN *in vivo* following NIHL is not clear.

In conclusion, we have shown that noise exposure that produces either a temporary or a permanent threshold shift causes changes in stellate cell mEPSCs. While the evidence suggests that both pre-and post-synaptic effects are likely to be involved, additional studies will be needed to identify the mechanisms involved. The dramatic increase in mEPSC frequency in TTS and PTS models could play a role in recruitment and could contribute to the generation of tinnitus. Nevertheless, further characterization of the mechanisms underlying the NIHL-induced sPESC changes we observed in stellate cells will be necessary to advance our understanding of the role of these cells in the pathophysiology of NIHL and tinnitus. The relationship of our findings in mouse to humans is somewhat unclear. It is not possible to perform the kinds of detailed analyses of synaptic transmission in the human cochlear nucleus that we have performed here. However, the cell complement in the cochlear nucleus has been noted to be quite similar in human and mouse27 39, and the responses of VCN neurons to sounds in lower mammals and primates are very similar14, thus it seems likely that the effects that we have seen may extend to humans.

Acknowledgments

Financial Support: This work was supported by grants from the National Institute on Deafness and other Communicative Disorders, T32DC005360 and R01 DC004551.

This work was supported by T32 DC005360 (AWR) and R01 DC004551 (PBM, RX) from the National Institute on Deafness and other Communication Disorders.

References

1. Quaranta, A. Noise Induced Hearing Loss: Basic Mechanisms, Prevention and Control. London: NRN Publications; 2001.
2. Nicolas-Puel C, Faulconbridge RL, Guitton M, Puel JL, Mondain M, Uziel A. Characteristics of tinnitus and etiology of associated hearing loss: a study of 123 patients. The international tinnitus journal. 2002; 8:37–44. [PubMed: 14763234]
3. Liberman MC. Single-neuron labeling and chronic cochlear pathology. I. Threshold shift and characteristic-frequency shift. Hearing research. 1984; 16:33–41. [PubMed: 6096345]

4. Sakaguchi H, Tokita J, Muller U, Kachar B. Tip links in hair cells: molecular composition and role in hearing loss. Current opinion in otolaryngology & head and neck surgery. 2009; 17:388–93. [PubMed: 19633555]
5. Cant NB, Benson CG. Parallel auditory pathways: projection patterns of the different neuronal populations in the dorsal and ventral cochlear nuclei. Brain Res Bull. 2003; 60:457–74. [PubMed: 12787867]
6. Manis, PB. Biophysical Specializations of Neurons that Encode Timing. In: Dallos, P.; Oertel, D., editors. Audition. San Diego: Academic Press; 2008. p. 565-86.
7. Oertel D. Synaptic responses and electrical properties of cells in brain slices of the mouse anteroventral cochlear nucleus. J Neurosci. 1983; 3:2043–53. [PubMed: 6619923]
8. Rhode WS, Oertel D, Smith PH. Physiological response properties of cells labeled intracellularly with horseradish peroxidase in cat ventral cochlear nucleus. The Journal of comparative neurology. 1983; 213:448–63. [PubMed: 6300200]
9. Moore JK, Osen KK. The cochlear nuclei in man. Am J Anat. 1979; 154:393–418. [PubMed: 433789]
10. Moore JK. The human auditory brain stem: a comparative view. Hearing research. 1987; 29:1–32. [PubMed: 3654394]
11. Rhode WS, Smith PH. Encoding timing and intensity in the ventral cochlear nucleus of the cat. Journal of neurophysiology. 1986; 56:261–86. [PubMed: 3760921]
12. Willott JF, Parham K, Hunter KP. Comparison of the auditory sensitivity of neurons in the cochlear nucleus and inferior colliculus of young and aging C57BL/6J and CBA/J mice. Hearing research. 1991; 53:78–94. [PubMed: 2066290]
13. Winter IM, Palmer AR. Responses of single units in the anteroventral cochlear nucleus of the guinea pig. Hearing research. 1990; 44:161–78. [PubMed: 2329092]
14. Rhode WS, Roth GL, Recio-Spinoso A. Response properties of cochlear nucleus neurons in monkeys. Hearing research. 2010; 259:1–15. [PubMed: 19531377]
15. Rhode WS, Greenberg S. Encoding of amplitude modulation in the cochlear nucleus of the cat. Journal of neurophysiology. 1994; 71:1797–825. [PubMed: 8064349]
16. Laudanski J, Coombes S, Palmer AR, Sumner CJ. Mode-locked spike trains in responses of ventral cochlear nucleus chopper and onset neurons to periodic stimuli. Journal of neurophysiology. 2009
17. Shannon RV, Zeng FG, Kamath V, Wygonski J, Ekelid M. Speech recognition with primarily temporal cues. Science (New York, NY). 1995; 270:303–4.
18. Wang Y, Manis PB. Synaptic transmission at the cochlear nucleus endbulb synapse during age-related hearing loss in mice. J Neurophysiol. 2005; 94:1814–24. [PubMed: 15901757]
19. Lu Y, Harris JA, Rubel EW. Development of spontaneous miniature EPSCs in mouse AVCN neurons during a critical period of afferent-dependent neuron survival. Journal of neurophysiology. 2007; 97:635–46. [PubMed: 17079338]
20. Francis HW, Manis PB. Effects of deafferentation on the electrophysiology of ventral cochlear nucleus neurons. Hearing research. 2000; 149:91–105. [PubMed: 11033249]
21. Cao XJ, McGinley MJ, Oertel D. Connections and synaptic function in the posteroventral cochlear nucleus of deaf jerker mice. The Journal of comparative neurology. 2008; 510:297–308. [PubMed: 18634002]
22. Oertel D. Use of brain slices in the study of the auditory system: spatial and temporal summation of synaptic inputs in cells in the anteroventral cochlear nucleus of the mouse. J Acoust Soc Am. 1985; 78:328–33. [PubMed: 2993393]
23. Wu SH, Oertel D. Intracellular injection with horseradish peroxidase of physiologically characterized stellate and bushy cells in slices of mouse anteroventral cochlear nucleus. J Neurosci. 1984; 4:1577–88. [PubMed: 6726347]
24. Clements JD, Bekkers JM. Detection of spontaneous synaptic events with an optimally scaled template. Biophysical journal. 1997; 73:220–9. [PubMed: 9199786]
25. Zheng QY, Johnson KR, Erway LC. Assessment of hearing in 80 inbred strains of mice by ABR threshold analyses. Hearing research. 1999; 130:94–107. [PubMed: 10320101]

26. Gardner SM, Trussell LO, Oertel D. Time course and permeation of synaptic AMPA receptors in cochlear nuclear neurons correlate with input. J Neurosci. 1999; 19:8721–9. [PubMed: 10516291]
27. Oleskevich S, Walmsley B. Synaptic transmission in the auditory brainstem of normal and congenitally deaf mice. J Physiol. 2002; 540:447–55. [PubMed: 11956335]
28. Emptage NJ, Reid CA, Fine A. Calcium stores in hippocampal synaptic boutons mediate short-term plasticity, store-operated Ca2+ entry, and spontaneous transmitter release. Neuron. 2001; 29:197–208. [PubMed: 11182091]
29. Taniguchi N, Takada N, Kimura F, Tsumoto T. Actions of brain-derived neurotrophic factor on evoked and spontaneous EPSCs dissociate with maturation of neurones cultured from rat visual cortex. J Physiol. 2000; 527(Pt 3):579–92. [PubMed: 10990542]
30. Illing RB, Kraus KS, Meidinger MA. Reconnecting neuronal networks in the auditory brainstem following unilateral deafening. Hearing research. 2005; 206:185–99. [PubMed: 16081008]
31. Muly SM, Gross JS, Morest DK, Potashner SJ. Synaptophysin in the cochlear nucleus following acoustic trauma. Experimental neurology. 2002; 177:202–21. [PubMed: 12429223]
32. Kujawa SG, Liberman MC. Adding insult to injury: cochlear nerve degeneration after “temporary” noise-induced hearing loss. J Neurosci. 2009; 29:14077–85. [PubMed: 19906956]
33. McKay SM, Oleskevich S. The role of spontaneous activity in development of the endbulb of Held synapse. Hearing research. 2007; 230:53–63. [PubMed: 17590547]
34. Rubio ME. Redistribution of synaptic AMPA receptors at glutamatergic synapses in the dorsal cochlear nucleus as an early response to cochlear ablation in rats. Hearing research. 2006; 216–217:154–67.
35. Koerber KC, Pfeiffer RR, Warr WB, Kiang NY. Spontaneous spike discharges from single units in the cochlear nucleus after destruction of the cochlea. Experimental neurology. 1966; 16:119–30. [PubMed: 5922930]
36. White JA, Young ED, Manis PB. The electrotonic structure of regular-spiking neurons in the ventral cochlear nucleus may determine their response properties. Journal of neurophysiology. 1994; 71:1774–86. [PubMed: 8064348]
37. Cai S, Ma WL, Young ED. Encoding intensity in ventral cochlear nucleus following acoustic trauma: implications for loudness recruitment. J Assoc Res Otolaryngol. 2009; 10:5–22. [PubMed: 18855070]
38. Kaltenbach JA. The dorsal cochlear nucleus as a contributor to tinnitus: mechanisms underlying the induction of hyperactivity. Prog Brain Res. 2007; 166:89–106. [PubMed: 17956775]
39. Rubio ME, Gudsnuk KA, Smith Y, Ryugo DK. Revealing the molecular layer of the primate dorsal cochlear nucleus. Neuroscience. 2008; 154:99–113. [PubMed: 18222048]

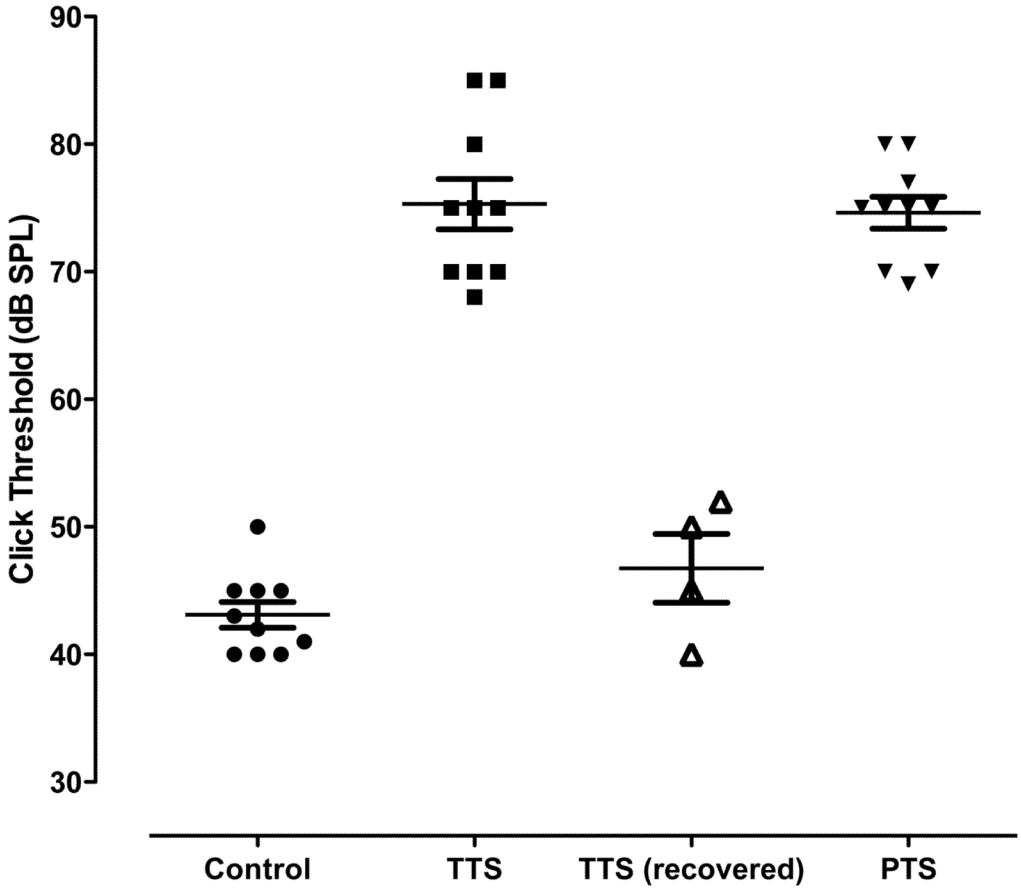

FIG. 1.

Click ABR thresholds were significantly increased in TTS and PTS mice when compared to the control group ($p<0.0001$), but recovered to control group thresholds in the TTS group 10–14 days after noise exposure ($p=0.0988$).

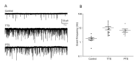

FIG. 2.

Spontaneous mEPSC event frequency in anteroventral cochlear nucleus (AVCN) stellate cells was significantly increased in TTS and PTS animals. A: representative mESPC traces from AVCN stellate cells from each group. Cells were held near their resting membrane potentials at −70 mV. B: Spontaneous mEPSC frequency was significantly higher in TTS and PTS mice than in the control group.

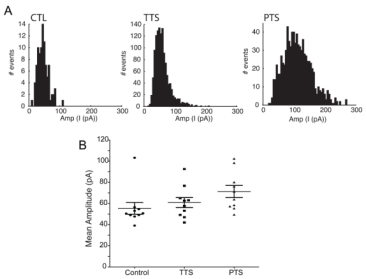

FIG. 3.

Spontaneous mEPSC amplitudes were significantly increased in PTS mice vs. control (p=0.037). A: Representative distribution patterns of mEPSC amplitudes in individual cells from each group. B: Spontaneous mEPSC amplitudes were significantly increased in PTS mice vs control animals, but was not significantly different from the TTS group (p=0.10)

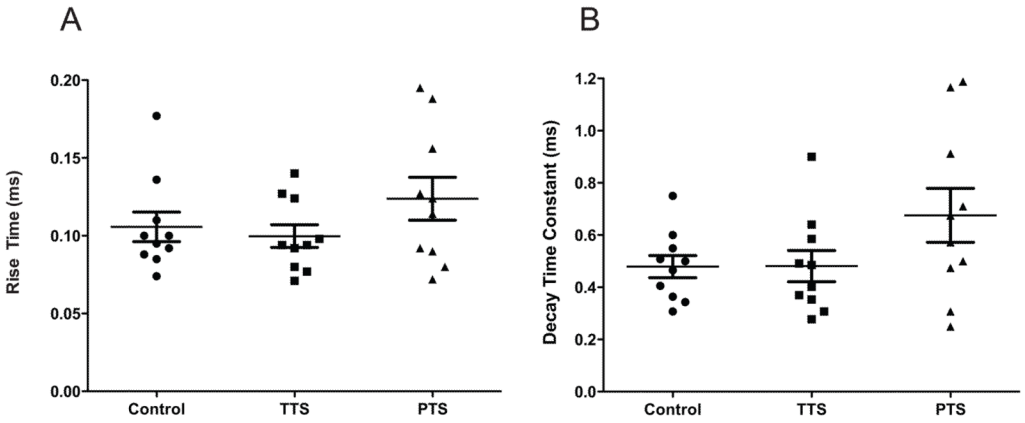

FIG. 4.

No significant difference in mEPSC time courses was noted between any of the experiment groups. A: No correlation in 10–90% rise time was seen between control, TTS, and PTS groups. B: No significant difference in mEPSC time constants was noted between any of the experiment groups.